Optimization of n/i and i/p buffer layers in n–i–p hydrogenated microcrystalline silicon solar cells*

Yuan Yujie(袁育杰)[1,2,3,†], Hou Guofu(侯国付)[1,2,3], Zhang Jianjun(张建军)[1,2,3], Xue Junming(薛俊明)[1,2,3], Cao Liran(曹丽冉)[1,2,3], Zhao Ying(赵颖)[1,2,3], and Geng Xinhua(耿新华)[1,2,3]

(1 Institute of Photoelectronics, Nankai University, Tianjin 300071, China)
(2 Tianjin Key Laboratory of Photoelectronic Thin Film Devices and Technology, Tianjin 300071, China)
(3 Key Laboratory of Optoelectronic Information Science and Technology, Chinese Ministry of Education, Tianjin 300071, China)

Abstract: Hydrogenated microcrystalline silicon (μc-Si:H) intrinsic films and solar cells with n–i–p configuration were prepared by plasma enhanced chemical vapor deposition (PECVD). The influence of n/i and i/p buffer layers on the μc-Si:H cell performance was studied in detail. The experimental results demonstrated that the efficiency is much improved when there is a higher crystallinity at n/i interface and an optimized a-Si:H buffer layer at i/p interface. By combining the above methods, the performance of μc-Si:H single-junction and a-Si:H/μc-Si:H tandem solar cells has been significantly improved.

Key words: microcrystalline silicon; interface; buffer layer; n–i–p solar cells
DOI: 10.1088/1674-4926/30/3/034007 **PACC:** 8115H; 8630J; 6855

1. Introduction

Hydrogenated microcrystalline silicon (μc-Si:H) thin films and solar cells have attracted much attention because of their better stability and higher red & infrared sensitivity than a-Si:H[1,2]. As well known that superior material quality in all the layers of a device is essential, but high quality material is not enough to achieve the high efficiency solar cell. An optimized cell design is also very important[3]. For a μc-Si:H n–i–p solar cell, we need to not only optimize the material quality for each layer, but also control the interface between layers[4]. For this purpose, we have done a systematic study of n/i and i/p buffer layers and their influence on the μc-Si:H cell performance.

In order to maintain similar material properties along the growth direction, a multi-step gradient hydrogen dilution technique has been adopted to control the microstructure evolution of the intrinsic layer in μc-Si:H solar cells[5]. The hydrogen dilution ratio and deposition time for every step during the fabrication of the whole intrinsic layer were varied in a wide range. Raman data show that the microcrystalline evolution was effectively controlled.

2. Experiment

The μc-Si:H intrinsic films and solar cells with n–i–p configuration were prepared in an in-line seven-chamber glow discharge system at a plasma excitation frequency of 13.56 MHz. A high-pressure-depletion condition has been adopted for the intrinsic layers[6]. Typical deposition parameters are: base pressure of the vacuum chamber $p_{\rm base} < 2.7\times10^{-4}$ Pa, deposition pressure $p = 3$ Torr, applied plasma power $P = 60$ W, and substrate temperature $T_{\rm s} = 175$ °C. A gas purifier was used to avoid incorporation of detrimental oxygen contamination. These conditions lead to deposition rate of ~2 A/s.

In order to ensure that there is the same pre-seed layer during the film deposition and device fabrication, an n-type μc-Si:H coated Glass / SnO_2 / ZnO was used as substrate to study the structural property of intrinsic μc-Si:H film. The sample structure is illustrated in Fig. 1. A series of intrinsic films with different thicknesses ranging from 50 to 1000 nm were prepared for structural property research. Raman scattering measurements were carried out with a micro-Raman Renishaw spectrophotometer equipped with a cooled CCD detector and an argon laser excitation at 514 nm. The crystalline volume fraction ($X_{\rm c}$) of a sample is defined as $X_{\rm c} = (I_{500} + I_{520}) / (I_{480} + I_{500} + I_{520})$, in which $I_{500} + I_{520}$ is attributed to crystalline grains (at 500 and 520 $\rm cm^{-1}$) and I_{480} is disordered regions (480 $\rm cm^{-1}$).

The μc-Si:H single junction n–i–p solar cells were

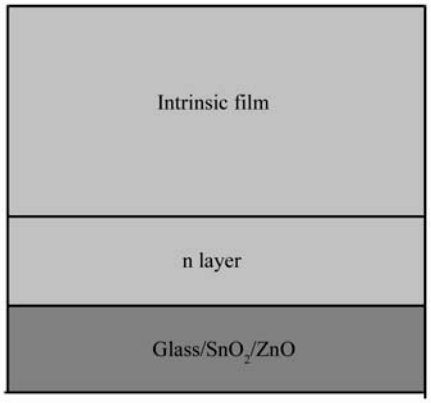

Fig. 1. Schematic of the sample structure.

* Project supported by the State Key Development Program for Basic Research of China (Nos. 2006CB202602, 2006CB202603) and the Tianjin Assistant Foundation for the National Basic Research Program of China (No. 07QTPTJC29500).
† Corresponding author. Email: yjyuan@mail.nankai.edu.cn
Received 25 June 2008, revised manuscript received 5 November 2008

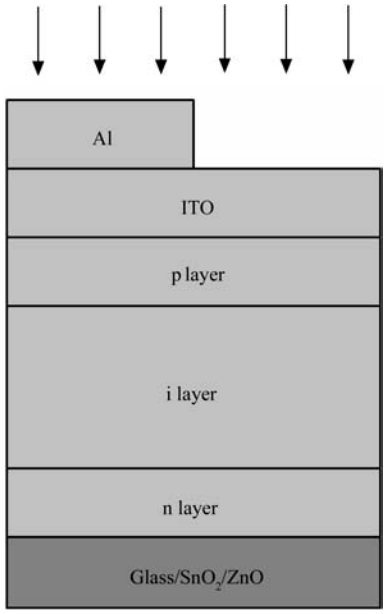

Fig. 2. Schematic of the solar cell structure.

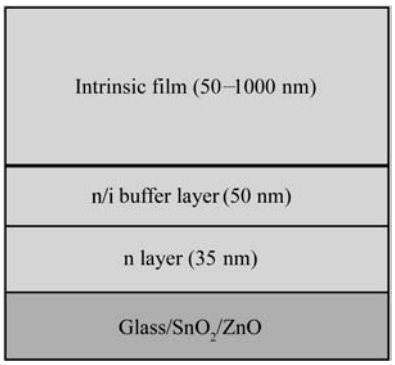

Fig. 3. Schematic of the sample (with n/i buffer layer) structure.

also fabricated to investigate the relationship between the devices and intrinsic films. Solar cells were constructed in the n–i–p sequence using Glass/SnO_2/ZnO as substrate. ITO/Al deposited on the p layer served as the top contact and defined the solar cell area of 0.18 cm^2. The solar cell structure is illustrated in Fig. 2. The solar cell performance was characterized by current density versus voltage (J–V) measurements under AM1.5 illumination (100 mW/cm^2). Quantum efficiency (QE) measurement was carried out with no optical bias for single-junction cells.

3. Results and discussion

3.1. Effect of n/i buffer layer on the structural properties of intrinsic films

In order to investigate the effect of n/i buffer layer on the structural properties of μc-Si:H intrinsic films, Glass / SnO_2 / ZnO coated with an n-type μc-Si:H layer was used as the substrate, four kinds of n/i buffer layers with different hydrogen dilution ratios ($R_{n/i}$) were deposited on the n-type layers, and on the top of each kind of n/i buffer layer, a series of intrinsic films were deposited with different thicknesses ranging from 50 to 1000 nm under the same condition for structural property research. The sample structure is illustrated in Fig. 3.

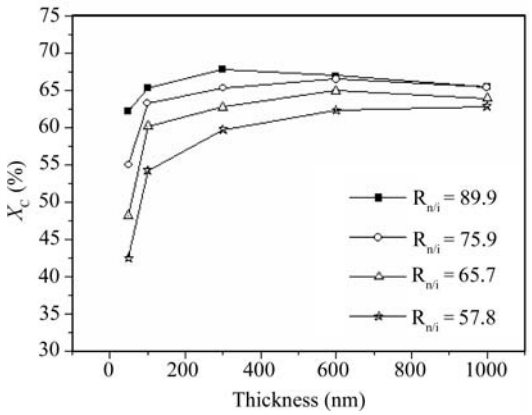

Fig. 4. X_c as a function of thickness for various n/i buffer layers.

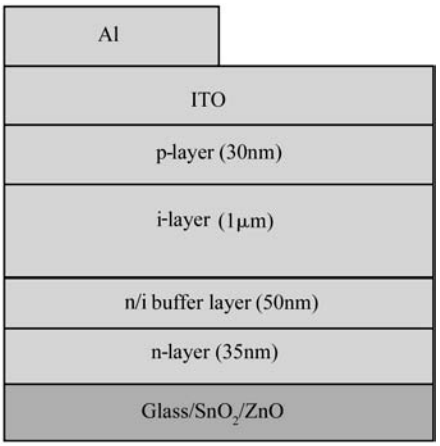

Fig. 5. Schematic of the solar cell (with n/i buffer layer) structure.

The crystalline volume fraction of intrinsic μc-Si:H films was measured using Raman spectroscopy with 514 nm Argon laser excitation. Figure 4 shows the crystalline volume fraction estimated from decomposition of the Raman spectra for intrinsic films with different thicknesses.

We employed the depth-profiled Raman spectroscopy to investigate the gradient in film crystallinity. Figure 4 shows the crystallinity profiles of μc-Si:H intrinsic films deposited with different n/i buffer layers. We can see that the μc-Si:H structure evolution become more inhomogeneous with $R_{n/i}$ decreasing from 89.9 to 57.8. For these four series of intrinsic films, we have adopted the same condition to deposit them, thus the difference of their structural properties along the growth direction must be caused by the n/i buffer layers. From Fig. 4, we also can see that the n/i buffer layer strongly affect the initial stage of intrinsic film, especially the first 300 nm. This could be explained by the underlying layer that influences the nucleation and microstructure of the subsequent layer.

3.2. Effect of n/i buffer layer on the performance of n–i–p μc-Si:H solar cells

Solar cells are very sensitive to changes in structural or optoelectronic properties of the μc-Si:H film. Therefore, μc-Si:H n–i–p solar cells were fabricated to evaluate the qualities of intrinsic μc-Si:H layers deposited with an i-layer thickness of 1.0 ± 0.1 μm. SnO_2/ZnO coated glass substrates served as back contacts, while ITO/Al deposited on the p-layer served as

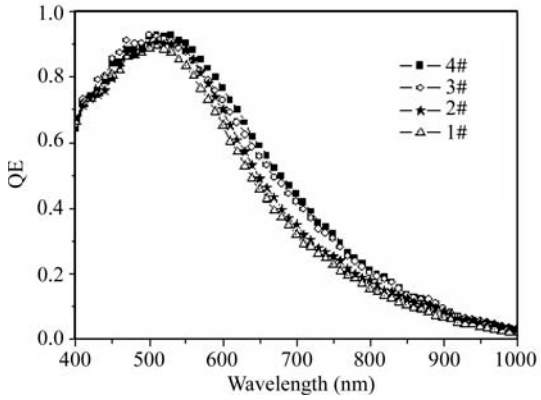

Fig. 6. Quantum efficiencies of solar cells with various n/i buffer layers. The sample number is listed in Table 1.

Table 1. *J–V* characteristics of μc-Si:H solar cells with different hydrogen dilution ratios for the first 50 nm.

Sample No.	n/i buffer layer R	V_{oc} (V)	J_{sc} (mA/cm^2)	FF (%)	η (%)
1#	57.8	0.438	17.75	53.40	4.15
2#	65.7	0.431	18.81	52.00	4.22
3#	75.9	0.424	19.88	51.30	4.33
4#	89.9	0.420	20.17	51.27	4.34

the top contact and defined the solar cell area of 0.18 cm^2. The deposition conditions for n-layer and i-layer were the same as those of samples in Fig. 3. The cell structure is illustrated in Fig. 5.

Table 1 shows the solar cell properties obtained with various n/i buffer layers. It is observed that short-circuit current density (J_{sc}) increases, but open circuit voltage (V_{oc}) and fill factor (FF) decrease as $R_{n/i}$ increases from 57.8 to 89.9. The higher J_{sc} and lower V_{oc} indicate a higher average microcrystalline volume fraction in i-layer (see Fig. 4).

Figure 6 plots the quantum efficiencies for the four n–i–p solar cells above. We found that for μc-Si:H n–i–p solar cells, an optimized n/i buffer layer can improve spectral response in the middle and long wavelength regions, hence increasing J_{sc}.

3.3. Effect of i/p buffer layer on the structural properties of intrinsic films

The i/p interface is critical for n–i–p solar cells, since more carriers are generated in this region, and the holes have to pass through this region to be collected[7]. From Table 1, we can see that the J_{sc} of solar cells is much improved by optimizing n/i buffer layer, but the V_{oc} and FF are still very poor, mainly because of the defect density in intrinsic layers, which could be related to the higher crystalline volume fraction with larger grain sizes and thus caused poor grain boundary passivation. In order to suppress this problem and improve the performance of n–i–p μc-Si:H solar cells, we have inserted a-Si:H layers that is defined as i/p buffer layer into the i/p interfaces of solar cells.

To investigate the effect of i/p buffer layers on the structural properties of μc-Si:H i-layers, Glass/SnO_2/ZnO coated

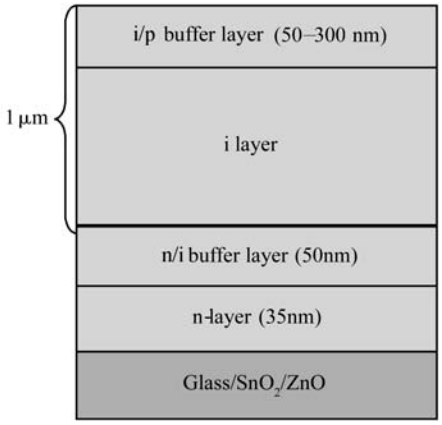

Fig. 7. Schematic of the solar cell (with i/p buffer layer) structure.

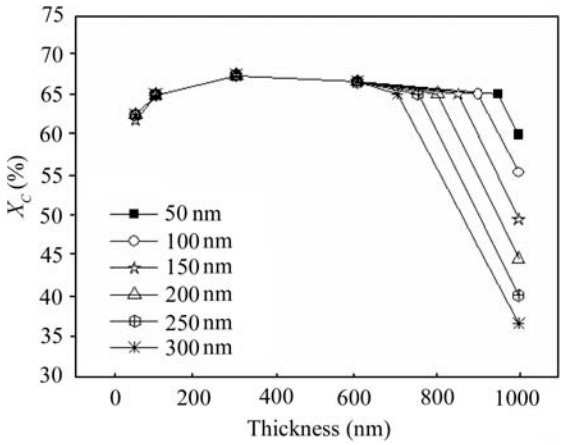

Fig. 8. X_c as a function of thickness for various i/p buffer layers.

with an n-type μc-Si:H layer was used as the substrate, and intrinsic films were deposited under the same condition on the n-type layers. Six kinds of a-Si:H i/p buffer layers with different thicknesses were deposited on the i-layers. The total thickness of i-layer and i/p buffer layer is 1 μm. The sample structure is illustrated in Fig. 7.

Figure 8 shows the crystallinity profiles of μc-Si:H intrinsic films deposited with various i/p buffer layers. We can see that the X_c at i/p interface decreases as the thickness of i/p buffer layer increases from 50 to 300 nm. Indeed, taking into account of Raman imaging microscope used here, the Raman collection depths (RCD) for μc-Si:H film is only 120–170 nm, but for the samples in which a-Si:H i/p buffer layer is thicker than 170 nm, there still exhibits a peak centred around 520 cm^{-1}. This could be explained by the epitaxy growth of i/p buffer layer deposited on highly crystallized i-layer, and the deposition condition of such a-Si:H buffer layer is just similar to the μc-Si:H / a-Si:H transition region.

3.4. Effect of i/p buffer layer on the performance of n–i–p μc-Si:H solar cells

Table 2 shows the solar cell properties obtained with various i/p buffer layers. The deposition conditions for intrinsic μc-Si:H films were similar to those of samples in Fig. 7. The cell structure is illustrated in Fig. 9. It is observed that J_{sc} remains around 20 mA/cm^2, but V_{oc} and FF significantly increase as the thickness of i/p buffer layer increases from 50

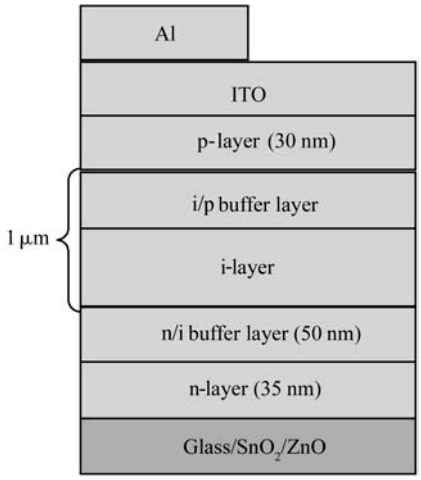

Fig. 9. Schematic of the solar cell (with i/p buffer layer).

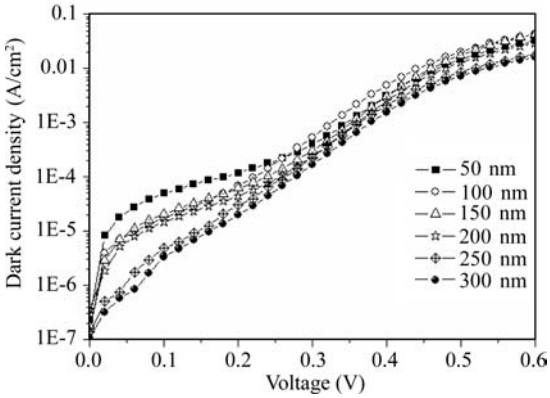

Fig. 10. Dark J–V characteristics of the solar cells structure made with various i/p buffer layers.

to 300 nm. The increased V_{oc} is due to the lower shunt current shown in Fig. 10. It is very common to have a high shunt current for μc-Si:H solar cells if there is no specific treatment on the interface[7]. Although the mechanism of a high shunt current is not very clear, controlling i/p interface can significantly reduce the shunt current. The dark J–V curves in Fig. 10 show a high shunt current at low voltages and level off at high voltages.

3.5. Optimization of n–i–p μc-Si:H single-junction and a-Si:H / μc-Si:H tandem solar cells

By optimizing the material quality for each layers and controlling the interfaces between layers, we have achieved an initial efficiency of 5.7% on the Al/Glass/SnO_2/ZnO substrate and 5.3% on the specular stainless steel substrate for μc-Si:H single-junction solar cells. Figure 11 shows the J–V characteristics and the quantum efficiencies of the best μc-Si:H single-junction cells with different substrates. From Fig. 11(a), we can see that the short circuit current density J_{sc} of the cell deposited on specular ss substrate is much lower than that on the Al/Glass/SnO_2/ZnO substrate. This phenomenon can be explained by the quantum efficiencies of the cells: from Fig. 11(b), we can see that the solar cell deposited on the Al/Glass/SnO_2/ZnO substrate has a significant response in the long wavelength region, which would be beneficial for improving J_{sc}. However the solar cell deposited on the specular ss substrate without Ag/ZnO back reflector has a much lower response in the long wavelength region, hence lowering J_{sc}.

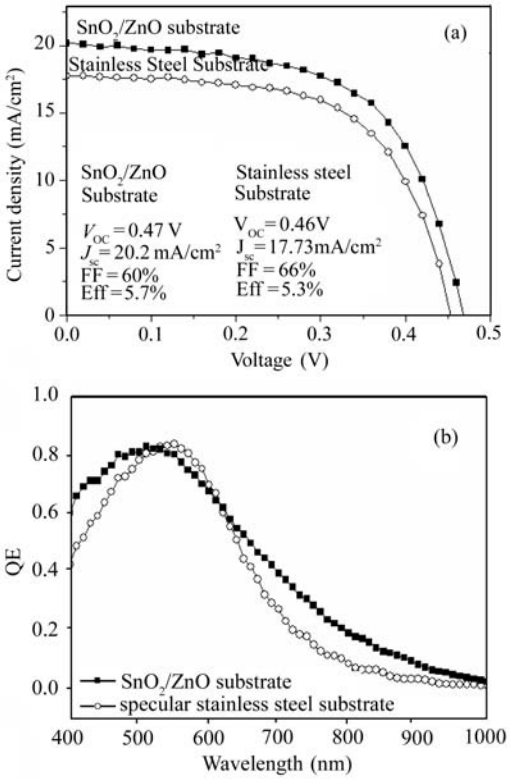

Fig. 11. (a) J–V characteristics and (b) quantum efficiencies of the best μc-Si:H single-junction cells made with different substrates.

Table 2. J–V characteristics of μc-Si:H single-junction solar cells with various i/p buffer layers.

Sample No	i/p buffer layer thickness	V_{oc} (V)	J_{sc} (mA/cm^2)	FF (%)	η (%)
5#	50 nm	0.42	19.86	51.46	4.30
6#	100 nm	0.44	20.31	51.90	4.64
7#	150 nm	0.43	20.55	51.94	4.59
8#	200 nm	0.44	20.68	51.65	4.70
9#	250 nm	0.45	20.27	55.58	5.07
10#	300 nm	0.47	20.04	58.00	5.50

By optimizing the current mismatch, we have achieved an initial efficiency of 10.12% on the Al/Glass/SnO_2/ZnO substrate and 9.15% on the specular stainless steel substrate for a-Si:H/μc-Si:H tandem cells. Figure 12 shows the J–V characteristics of the best a-Si:H/μc-Si:H tandem cells with different substrates.

4. Conclusion

This paper summarizes our recent studies of the interface dependence of the cell performance. While high quality material is an essential condition for achieving high efficiency solar cells, an optimized cell design is also very important. Controlling the interfaces between the doped layers and the i-layer is especially critical for solar cell optimization. We find that

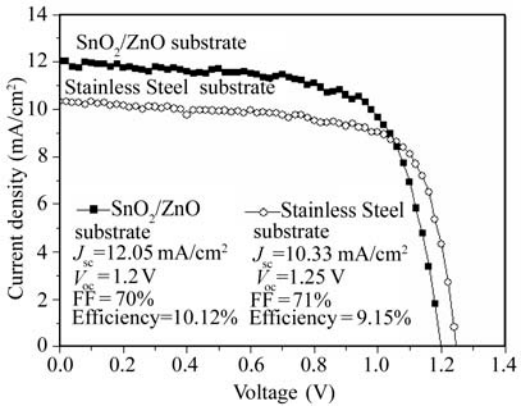

Fig. 12. *J-V* characteristics of the best a-Si:H/μc-Si:H tandem cells made with different substrates.

an optimized n/i buffer layer can improve spectral response in the middle and long wavelength regions, hence increasing the short-circuit current density; an optimized i/p buffer layer significantly reduces the shunt current, hence increasing the open circuit voltage.

To date, we have achieved an initial efficiency of 5.7% on the Al/Glass/SnO_2/ZnO substrate and 5.3% on the specular stainless steel substrate for μc-Si:H single-junction solar cells. We have also achieved an initial efficiency of 10.12% on the Al/Glass/SnO_2/ZnO substrate and 9.15% on the specular stainless steel substrate for a-Si:H/μc-Si:H tandem cells.

References

[1] Meier J, Dubail S, Platz R, et al. Towards high-efficiency thin-film silicon solar cells with the "micromorph" concept. Solar Energy Materials and Solar Cells, 1997, 49(1–4): 35

[2] Vetterl O, Finger F, Carius R, et al. Intrinsic microcrystalline silicon: a new material for photovoltaics. Solar Energy Materials and Solar Cells, 2000, 62(1/2): 97

[3] Rech B, Repmann T, Donker M, et al. Challenges in microcrystalline silicon based solar cell technology. Thin Solid Films, 2006, 511/512: 548

[4] Yan B, Yue G, Guha S. Status of nc-Si:H solar cells at united solar and roadmap for manufacturing a-Si:H and nc-Si:H based solar panels. Mater Res Soc Symp Proc, 2007, 989: A15.1

[5] Hou G F, Xue J M, Guo Q C, et al. Formation mechanism of incubation layers in the initial stage of microcrystalline silicon growth by PECVD. Chinese Physics, 2007, 16: 553

[6] Hou G F, Xue J M, Yuan Y J, et al. A fast method to diagnose phase transition from amorphous to microcrystalline silicon. Sci China Ser G-Phys Mech Astron, 2007, 50: 731

[7] Yan B, Yue G, Yang J, et al. Hydrogen dilution profiling for hydrogenated microcrystalline silicon solar cells. Appl Phys Lett, 2004, 85: 1955